THE EFFECT OF SHALLOW CUMULUS CONVECTION ON THE SEGREGATION OF CHEMICAL REACTANTS

Si-Wan Kim, Mary C. Barth, Chin-Hoh Moeng

National Center for Atmospheric Research
Boulder, Colorado, USA

1. INTRODUCTION

Chemical reaction in the atmospheric boundary layer can be controlled by the turbulent mixing as well as chemical reactivity (Schumann, 1989, Sykes et al., 1994, Petersen et al., 1999, Krol et al., 2000, Patton et al., 2001). If the chemical reaction rate is faster than or equal to turbulent mixing rate, the reaction rates of species will be affected by the turbulent mixing. Schumann (1989) and Sykes et al. (1994) in their LES of simple binary reactions have shown that turbulence in the convective boundary layer (CBL) segregated top down (e.g. ozone) and bottom up (e.g. nitric oxide) reactive scalars and retarded reaction rates significantly. Krol et al. (2000) in their LES of photochemical reactions (6 species, 10 reactions) indicated that segregation between generic hydrocarbon and hydroxyl radical (OH) reaches ~7% (~30%) when homogenous (inhomogeneous) emission was considered. Recently the effect of turbulence on the segregation between surface-emitted biogenic hydrocarbons and in-situ produced oxidants has been investigated since chemical time scale of isoprene or α-pinene is the same order of turbulent mixing time scale in the CBL. Barth et al. (2004) demonstrated that reaction rates between isoprene and OH may be reduced by 5% ~ 50% in the LES of clear CBL depending on the chemical scenario (38 species, 124 reactions).

Fair-weather cumuli are abundant during summertime under high pressure system when photochemical reactions and isoprene emission are at their greatest. Previous studies have not addressed the effect of fair weather cumulus clouds on chemical reactivity. In this study we use a LES model to examine the effects of fair-weather cumuli, turbulence dynamics, and aqueous-phase chemistry on the segregation of isoprene and OH.

2. MODEL DESCRIPTION

The LES code is configured for the conditions observed at the Southern Great Plains site of the Atmospheric Radiation Measurement program on 21 June 1997. The chemistry mechanism used in this study is similar to the mechanism used in the NCAR HANK model, but is updated following the NCAR global chemical transport model MOZART2.2. The mechanism contains 141 gas-phase reactions and 29 aqueous-phase reactions for which 54 species are predicted. The gas chemistry represents daytime chemistry of methane (1700 ppbv), carbon monoxide (200 ppbv), ozone, odd nitrogen species, peroxides, aldehydes, non-methane hydrocarbons (ethane, ethene, propylene, isoprene, α-pinene), methyl vinyl ketone (MVK), methacrolein (MACR), sulfur dioxide, peroxy radicals, formic acid, and peracetic acid. The aqueous chemistry is computed for the cloud water assuming a pH of 5.0. Chemical species with short chemical lifetimes are initialized with a photochemical box model, which is integrated from midnight to 0830 LST (local standard time), using chemical conditions measured during the PROPHET (Faloona et al., 2001, Westberg et al. 2001) field experiment. Surface emissions of key biogenic hydrocarbons, isoprene (maximum 5.04 mg m^{-2} hr^{-1}) and a-pinene (maximum 0.504 mg m^{-2} hr^{-1}), follow a diurnal-cycle profile, while that of nitric oxide is a constant value (0.18 mg NO m^{-2} hr^{-1}). The dynamics, cloud physics, and chemistry are integrated over a model domain of 6.4 km x 6.4 km x 4.4 km (with 96 x 96 x 96 grid points) with periodic boundary conditions in x and y. The simulation of the dynamics and physics begins at 0530 LST, while the simulation of the chemistry begins at 0830 LST when the turbulent flow is established and cumulus cloud starts to form. The whole simulation time with chemistry is 6 hours. The chemical mechanism is solved with an Euler backward iterative approximation using a Gauss-Seidel method with variable iterations. A convergence criterion of 0.01% is used for all the species.

3. RESULTS

Vertical profiles of meteorological variables show the development of cloudy boundary layer. The evolution of clouds are exhibited in Fig. 1. Clouds are formed at 0830 LST. Cloud fraction increased with time and reached maximum 0.4 at 1130 LST. After this time, it decreased to 0.2 at 1430 LST. Cloud base increased slowly by surface heating and cloud top increased more rapidly to about 3000 m.

To highlight the effect of aqueous chemistry on the segregation of isoprene and OH, two simulations are performed; one with only gas-phase chemistry and one with both gas and aqueous-phase chemistry. The horizontally-averaged concentrations of isoprene and OH show nearly identical vertical profiles for both simulations. Mean isoprene concentrations decrease with height with strong gradients occurring near the surface where isoprene is emitted and across the cloud layer. Mean OH concentrations are nearly constant (0.2 pptv) with height in the mixed layer, increase in the cloud layer to ~0.8 pptv, and decrease above the cloud layer.

The horizontally-averaged variance of isoprene shows a nearly identical vertical profile for the two simulations, while the OH variance does not (Fig. 2). Variance of OH is the greatest in the cloud layer. Convection by shallow cumulus clouds increases OH variance in the cloud layer. Furthermore, aqueous phase chemistry enhances OH variance significantly.

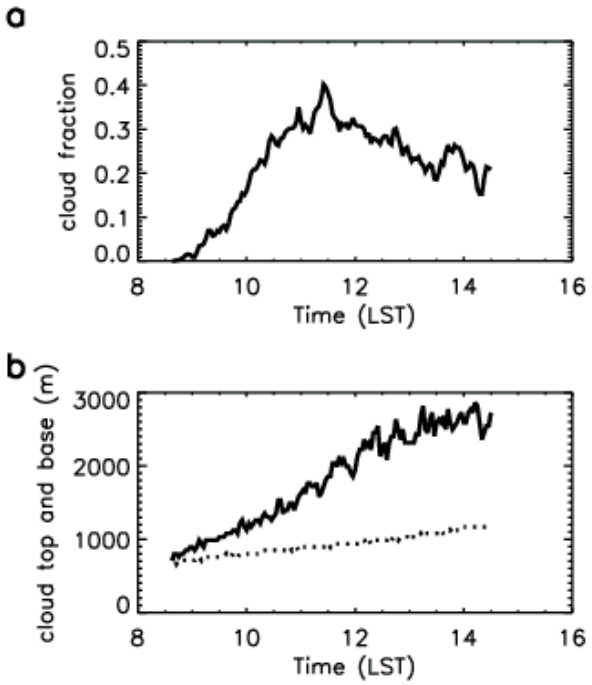

Figure 1. The evolution of (a) cloud fraction and (b) cloud top (solid line) and base (dotted line). LST denotes local standard time.

Intensity of segregation between isoprene and OH is defined as

$$I_s = \frac{\left\langle \overline{(C_5H_8)'(OH)'} \right\rangle}{\left\langle \overline{C_5H_8} \right\rangle \left\langle \overline{OH} \right\rangle}, \qquad (1)$$

where the overline denotes horizontal average, prime indicates fluctuation from horizontal average and angle brackets represent time average. The intensity of segregation indicates the degree of segregation between two species. If I_s = -1, the two species are completely segregated.

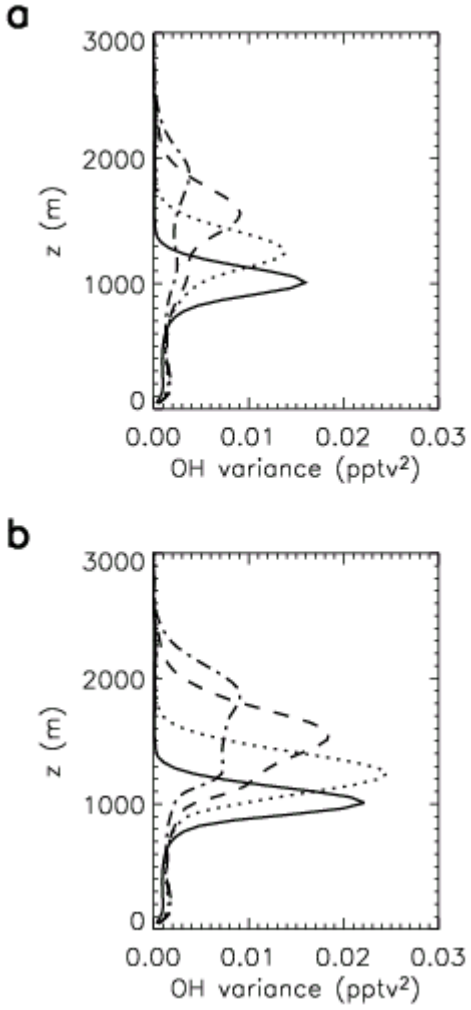

Figure 2. Profiles of variance of OH for (a) gaseous phase chemistry and (b) gas and aqueous phase chemistry. Solid, dotted, dashed, and dash-dotted lines represent 1100LST, 1200LST, 1300LST, and 1400LST, respectively.

Fig. 3 shows the intensity of segregation defined by Eq. (1) for cases with and without aqueous phase chemistry. Without aqueous chemistry, segregation reaches 30% to 15% in the cloud layer, which is greater than those in clear convective boundary layer under similar chemical scenario (Barth et al., 2004). Aqueous chemistry enhances further the segregation up to 40%.

To understand the effect of chemistry on the intensity of segregation, we examine each term in the covariance budget of $\left\langle \overline{(C_5H_8)'(OH)'} \right\rangle$, which is shown as

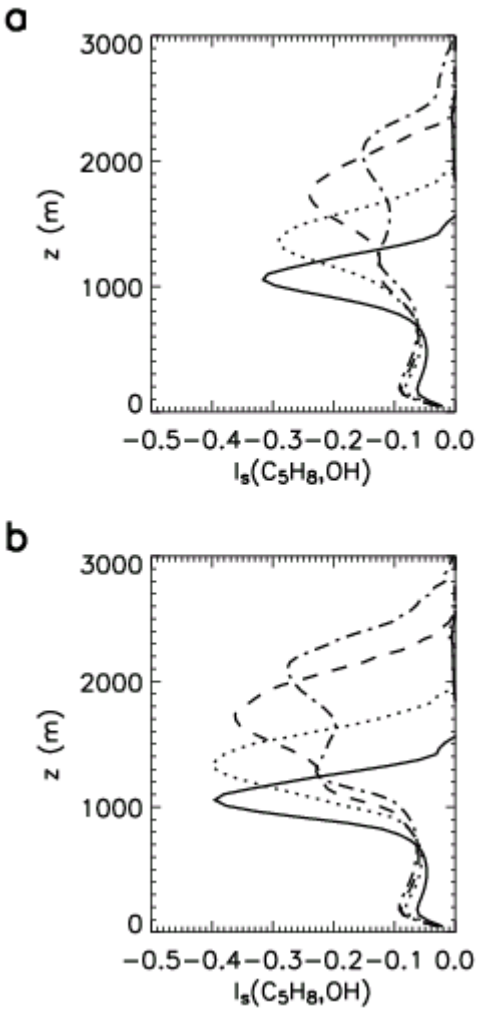

Figure 3. Profiles of intensity of segregation I_s between isoprene and OH for (a) gaseous phase chemistry and (b) gas and aqueous phase chemistry. Solid, dotted, dashed, and dash-dotted lines represent 1100LST, 1200LST, 1300LST, and 1400LST, respectively.

$$\partial \left\langle \overline{(C_5H_8)'(OH)'} \right\rangle / \partial t = - \left\langle \overline{w'(C_5H_8)'} \right\rangle \partial \left\langle \overline{OH} \right\rangle / \partial z - \left\langle \overline{w'(OH)'} \right\rangle \partial \left\langle \overline{C_5H_8} \right\rangle / \partial z - \partial \left\langle \overline{w'(C_5H_8)'(OH)'} \right\rangle / \partial z - \left\langle \overline{(C_5H_8)'(\partial \tau_{wOH} / \partial z)} \right\rangle - \left\langle \overline{(OH)'(\partial \tau_{wC5H8} / \partial z)} \right\rangle + \partial \left\langle \overline{(C_5H_8)'(OH)'} \right\rangle / \partial t \Big|_{chem} \quad (2)$$

where the first two terms on the right hand side are gradient production terms, the third term is turbulent transport term, the fourth and the fifth terms are subgrid scale (SGS) diffusion process, and the last term is chemical reaction process. In this study, the chemical reaction process term is derived as the residual of Eq. (2). Fig. 4 demonstrates the magnitude of each term in the covariance budget equation. Temporal change of covariance is negligible compared to other processes. Gradient production terms are negative for the whole layer, which enhances the segregation of species. Near the surface, turbulent transport and chemical reaction processes also increase segregation of the species, but SGS diffusion process tends to increase positive correlation. When aqueous phase chemistry is not included (Fig. 4a), chemical reaction process increase the positive correlation between isoprene and OH in the cloud layer. Meanwhile, when aqueous phase chemistry is calculated (Fig. 4b), chemical reaction process tends to enhance segregation of the species in the cloud layer.

4. CONCLUSIONS

Our study shows that shallow cumulus convection and aqueous-phase chemistry can enhance the segregation of chemical reactants. When only gas-phase chemistry is included, the segregation of isoprene and OH, which reaches 30% in the cloud layer, is enhanced by the vertical gradient production of covariance. When gas and aqueous phase chemical reactions are included, the segregation of isoprene and OH is greater reaching 40% in the cloud layer. In addition to the gradient production of covariance, cloud chemistry contributes to the isoprene-OH segregation.

In this study, the chemical reaction process term was calculated as the residual in the covariance budget equation. To determine which chemical reaction is the dominant contributor to the covariance production or destruction, an explicit calculation of the covariance chemistry term will be performed and examined. The LES code developed here can be utilized to understand and

parameterize the effect of shallow cumulus clouds on the transport of chemical species, chemical reactivity, and radiation processes. Tests under various chemical scenarios and atmospheric conditions (e.g., marine boundary layer) are needed.

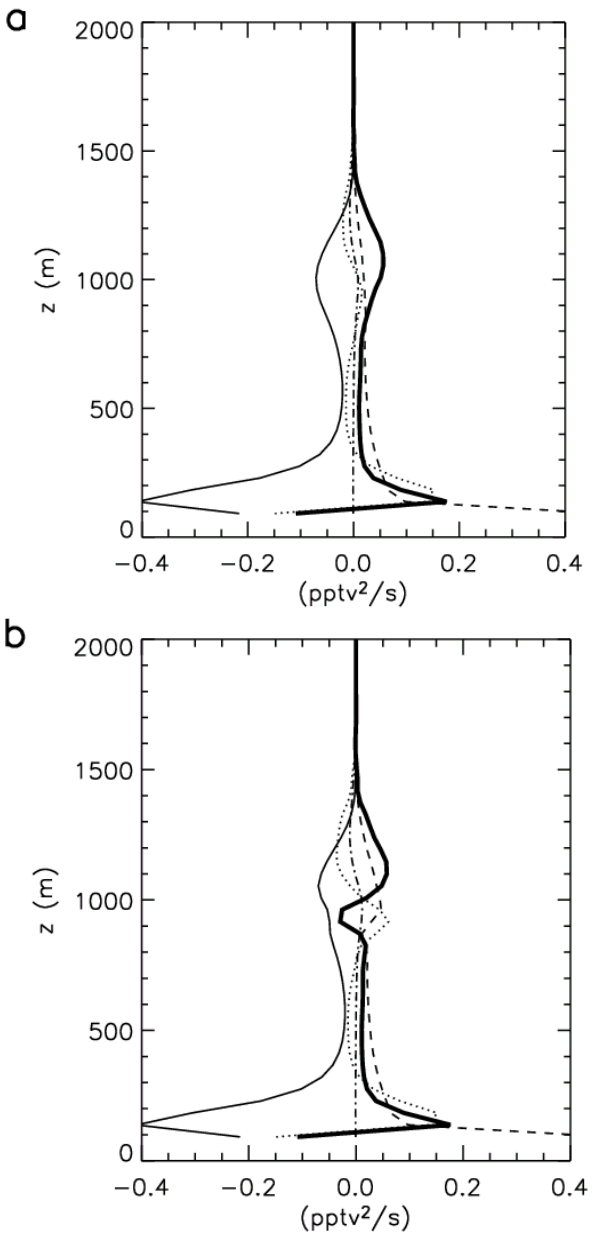

Figure 4. Profiles of covariance budget averaged over 1030LST to 1130LST. Solid lines stand for mean gradient term, dotted lines for turbulent transport term, dashed lines for subgrid-scale diffusion process, dash-dotted lines for tendency of covariance, and thick solid lines for the residuals which represent the chemical reaction process.

5. ACKNOWLEDGMENTS

The National Center for Atmospheric Research is operated by the University Corporation for Atmospheric Research under the sponsorship of the National Science Foundation.

6. REFERENCES

Barth et al., 2004: Large eddy simulations of isoprene chemistry in the convective boundary layer. *In preparation*.

Faloona et al., 2001: Nighttime observations of anomalously high levels of hydroxyl radicals above a deciduous forest canopy. *J. Geophys. Res.* **106**, 24,315-24,334.

Krol et al., 2000: Effects of turbulence and heterogeneous emissions on photochemically active species in the convective boundary layer. *J. Geophys. Res.* **105**, 6871-6884.

Patton et al., 2001: Decaying scalars emitted by a forest canopy: A numerical study. *Boundary-Layer Meteorol.*, 48, 91-129.

Petersen et al., 1999: Mass-Flux characteristics of reactive scalars in the convective boundary layer. *J. Atmos. Sci.,* **56**, 37-56.

Schumann, 1989: Large-Eddy Simulation of Turbulent diffusion with chemical reactions in the convective boundary layer. *Atmos. Environ*., **23**, 1713-1727.

Sykes et al., 1994: Turbulent mixing with chemical reaction in the planetary boundary layer. *J. Appl. Meteorol.,* **23**, 1713-1727.

Westberg et al., 2001: Measurement of isoprene fluxes at the PROPHET site. *J. Geophys. Res.* **106**, 24,347-24,358.